

> REPLACE THIS LINE WITH YOUR MANUSCRIPT ID NUMBER (DOUBLE-CLICK HERE TO EDIT) <

A Home-based Upper Limb Rehabilitation System via Cloud-based Teleoperation and sEMG-driven Bilateral Control

He Li, *Student Member, IEEE*, Shuxiang Guo, *Fellow, IEEE*, Ruijie He, *Student Member, IEEE*, Hanze Wang, *Student Member, IEEE*, and Masahiko Kawanishi

Abstract—With the growing number of patients suffering from upper limb hemiplegia, robot-assisted rehabilitation has attracted more and more attention. Compared to traditional face-to-face rehabilitation, telerehabilitation is an effective alternative with therapist-in-the-loop. Meanwhile, bilateral rehabilitation based on surface electromyography (sEMG) enables patients to train by themselves. Although numerous telerehabilitation or bilateral rehabilitation systems have been proposed, limited studies have addressed cloud communication and inter-subject variability. This paper proposes a home-based upper limb rehabilitation (HB-ULR) system utilizing cloud-based teleoperation and sEMG-based subject-independent bilateral control. In the cloud-based telerehabilitation (CBTR) subsystem, experiments with the master side in Beijing City (China) and the slave side deployed in three different cities are conducted through one cloud server. The slave side is controlled by the master side, while the contact force is transmitted back to the master side. In the sEMG-driven subject-independent bilateral rehabilitation (sEMG-SIBR) subsystem, continuous motion can be predicted by a model after transfer learning. The validity of transfer learning in solving inter-subject variability is verified by both offline and real-time experiments, with the prediction error kept within 10° . Therefore, the HB-ULR system integrating CBTR and sEMG-SIBR subsystems is built. It supports both routine tele-rehabilitation and daily self-training at home, offering significant potential for enhancing the recovery outcome.

Index Terms—Home-based upper limb rehabilitation (HB-ULR); Cloud-based teleoperation; Surface electromyography (sEMG); Transfer learning; Continuous motion prediction

This work was supported in part by the National Natural Science Foundation of China (61703305), in part by National High-tech Research and Development Program (863 Program) of China (2015AA043202), in part by SPS KAKENHI (15K2120). (Corresponding author: Shuxiang Guo)

H. Li, R. J. He, and H. Z. Wang are with the School of Life Science, Beijing Institute of Technology, Beijing 100081, China, also with the Key Laboratory of Convergence Biomedical Engineering System and Healthcare Technology, The Ministry of Industry and Information Technology, Beijing Institute of Technology, Beijing 100081, China (email: {lihe, heruijie, wanghanze}@bit.edu.cn).

S. X. Guo is with both the Department of Electronic and Electrical Engineering, Southern University of Science and Technology, Shenzhen, Guangdong 518055, China, and the Intelligent of Mechanical System Engineering Department, Kagawa University, Japan (email: guo.shuxiang@kagawa-u.ac.jp).

Masahiko Kawanishi is with the Department of Neurological Surgery, Faculty of Medicine, Kagawa University, Takamatsu 761-0793, Japan (email: mk@kms.ac.jp).

This research is approved by the Institutional Review Board (IRB) of Faculty of Engineering and Design, Kagawa University (Ref. No. 01-011 from February 2020).

I. INTRODUCTION

STROKE is a leading cause of hemiparesis, with 40–60% resulting in motor deficits in one of the upper extremities [1]. Upper limb hemiplegia profoundly affects patients' daily activities and significantly diminishes their quality of life. Timely and effective rehabilitation training can alleviate motor impairment and promote the recovery of motor function in the affected upper limb of hemiplegic patients [2]. Therefore, rehabilitation plays a crucial role in the recovery process of hemiplegic patients.

However, rehabilitation care is typically a long-term process. On the one hand, it imposes significant psychological and financial burdens on patients' families. On the other hand, the demand for stroke rehabilitation services is growing [3], as the increasing number of stroke survivors further intensifies the need for such services. Due to the lack of rehabilitation institutions and therapists, only a small number of stroke survivors can access professional rehabilitation services. In other words, traditional rehabilitation training brings a heavy burden on both families and healthcare systems. Robotic rehabilitation represents a promising approach to stroke rehabilitation [4]–[6]. Compared to conventional rehabilitation approaches, robotic systems offer substantial practical and cost-effective benefits. They can quantitatively assess rehabilitation outcomes and provide training consistently and repetitively, thereby freeing therapists from repetitive and tedious work. Therefore, rehabilitation robots are anticipated to play an essential role in future rehabilitation treatment [7]–[9].

Compared to traditional rehabilitation training that requires face-to-face interaction with a therapist, robot-assisted telerehabilitation [9] integrates rehabilitation robots with information technology and transmits evaluation data to therapists over the internet. Therefore, treatment can be transferred from one specialized facility to patients' homes under remote supervision by therapists. At the same time, it can reduce treatment costs, travel time to clinics, and the financial burden on patients. For post-stroke motor disabilities, Atashzar et al. [11] developed a haptics-enabled robotic neurorehabilitation system that incorporates a neural network-based supervised training framework. However, the slave-side equipment is not portable, and its high cost hinders its application in home-based telerehabilitation. Yi Liu et al. [4] developed a telerehabilitation system for home-based training,

> REPLACE THIS LINE WITH YOUR MANUSCRIPT ID NUMBER (DOUBLE-CLICK HERE TO EDIT) <

which was designed to enhance remote interaction between therapists and patients. However, its communication is restricted to a campus local area network (LAN). Based on motion tracking, Jing Bai et al. [12] proposed a cloud communication-based rehabilitation system for the upper limb. This system is based on virtual games, making it different from robot-assisted tele-rehabilitation systems. Yang et al. [13] presented a preliminary study based on cloud communication, focusing on interventional robots not rehabilitation robots. In this study, the combination of a haptic-enabled master device, cloud communication, and the exoskeleton device on the slave side is utilized in home-based upper limb telerehabilitation.

Bilateral training is widely adopted as a rehabilitation protocol for post-stroke motor impairments [14]. Bilateral therapy is based on the mirroring principle, in which the affected limb mimics the movement of the intact limb. This approach aims to enhance voluntary control over the impaired limb through synchronized bilateral movements. The surface electromyography (sEMG)-driven bilateral training is achieved by decoding the motor intention of the healthy side to control the affected side [15]. As a non-invasive measurement of the electrical activity of a muscle contraction, the sEMG signal has been widely used in the recognition of motion intention for exoskeletons and prostheses [16]. Yi Liu et al. [6] presented a home-based bilateral rehabilitation system with sEMG-based real-time variable stiffness control. In this system, a musculoskeletal model of the upper limb was adopted to decode the motion intention from sEMG signals. Since individuals differ in physiological parameters, personalized modeling is required for each patient. Ziyi Yang et al. [17] proposed an sEMG-based bilateral rehabilitation system for upper limb motor recovery. They adopted a neural network to predict the motion intention and trained subject-specific models due to the inter-subject variability. He Li et al. [5] built a robot-assisted system using a Convolutional Neural Network-Long Short-Term Memory (CNN-LSTM) architecture for subject-independent estimation. Although CNN can learn transferable features, this method fails to fully address the influence of inter-subject variability on motion intention prediction. Yassine Bouteraa et al. [18] designed and developed a new robotic system for upper limb rehabilitation, which integrates electrical stimulation into motor rehabilitation through robotic systems. This offers a complementary view to the use of sEMG in subject-independent bilateral control. In this study, transfer learning is further adopted to realize the subject-independent motion estimation, targeting the inter-subject variability.

In this paper, the home-based upper limb rehabilitation (HB-ULR) system based on cloud-based teleoperation and sEMG-driven subject-independent bilateral training is presented. The system employs a gear-driven powered upper limb exoskeleton (GP-ULE) as the slave-side device. The HB-ULR system comprises the cloud-based telerehabilitation (CBTR) subsystem and the sEMG-based subject-independent bilateral rehabilitation (sEMG-SIBR) subsystem. In the CBTR subsystem, the control commands from the therapist side to the robot-assisted side, as well as the force feedback from the robot-assisted side to the

therapist side, are transmitted through one cloud server. The therapist can remotely control the GP-ULE to drive the patients' affected limb and perceive the interaction force between the affected side and the robot to adjust the rehabilitation intensity. In the sEMG-SIBR subsystem, the affected limb is driven by the exoskeleton robot, which is controlled by sEMG signals from the intact limb. Transfer learning is used to realize the subject-independent estimation of motion intention. By integrating the two subsystems, the overall HB-ULR system is developed to support both therapist-supervised telerehabilitation and patients' self-rehabilitation training based on bilateral therapy. Thus, the regular telerehabilitation and daily home-based self-rehabilitation are realized. Regular tele-rehabilitation supervised by therapists can offer professional guidance that enhances the effectiveness of patients' home-based bilateral rehabilitation. The key innovations of this study lie in the development of a novel integrated rehabilitation system, as follows:

- (1) **CBTR**: Enables real-time remote operation with force feedback between therapists and patients, demonstrating the feasibility of long-distance telerehabilitation through cloud servers. This represents a novel application of cloud technology in the field of rehabilitation robotics, enabling scalable and accessible remote healthcare services.
- (2) **sEMG-SIBR**: Allows patients to perform autonomous rehabilitation exercises using sEMG signals from the unaffected limb. By combining a CNN-LSTM model with transfer learning, the system achieves cross-subject adaptability without requiring subject-specific calibration.

The rest of the paper is organized as follows. Section II describes the involved methods, which include the overview of the proposed robotic system for home-based rehabilitation, the commercial equipment, the exoskeleton design and control, the CBTR, and the sEMG-SIBR using transfer learning. The introduction of the experiments in this study is described in Section III. In Section IV, the results and discussion are shown. Section V is the conclusion.

II. METHODS

A. Overview of the Proposed Robotic System for Home-based Rehabilitation

Fig. 1 illustrates the overview architecture of the HB-ULR system, integrating the CBTR subsystem and the sEMG-SIBR subsystem. This system comprises the therapist side, the robot-assisted limb side, and the intact limb side. The therapist side and the robot-assisted limb side constitute the therapist-in-the-loop CBTR subsystem; the intact limb side and the robot-assisted limb side form the sEMG-SIBR subsystem. In both the CBTR subsystem and the sEMG-SIBR subsystem, the GP-ULE serves as the hardware platform for the affected side of patients.

In the CBTR subsystem, one user (serves as a therapist) operates the master-side device, and another user (serves as a patient with upper limb hemiplegia) wears the GP-ULE in the slave side. The data transmission between the master side and the slave side is realized through a cloud server. The motion

> REPLACE THIS LINE WITH YOUR MANUSCRIPT ID NUMBER (DOUBLE-CLICK HERE TO EDIT) <

control commands are transmitted from the therapist side to the robot-assisted side, while the contact force between the GP-ULE and the patient is fed back from the robot-assisted side to the therapist side in real time. In the sEMG-SIBR subsystem, the motor control of the affected side is realized by decoding the sEMG signal from the intact limb. The subject-independent motion estimation based on sEMG is achieved using transfer learning to the pre-trained CNN-LSTM model.

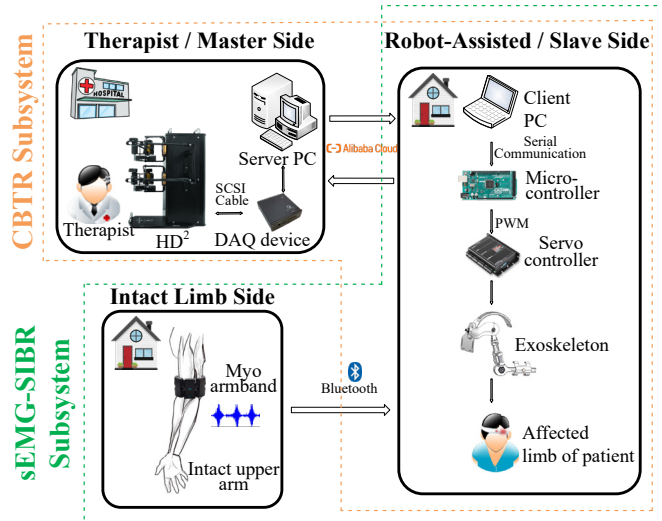


Fig. 1. The overview framework of the HB-ULTR system combining the CBTR platform and the sEMG-SIBR platform.

B. Commercial Equipment

The HD² High-Definition Haptic Device [19] (Quanser, Canada) is a high-fidelity robotic manipulator designed for haptic interaction with virtual or remote environments. Using seven high-resolution optical encoders, the operator's motion can be tracked in six degrees of freedom (DoFs), i.e., three translational motions in Cartesian space and three rotational motions (i.e., roll, pitch, and yaw). The system is connected to a computer via Quanser's superior hardware control board QID/QIDe and utilizes its Real-Time Control (QuRC) software compatible with MATLAB/Simulink (2022b, MathWorks).

The Myo armband (Thalmic Labs, Canada) is used for sEMG acquisition in this study. The armband comprises eight "medical-grade" stainless-steel sEMG sensors, which are held together through an expandable flex band. The band also comes with sizing clips that can be adjusted to ensure it fits the forearm properly. Equipped with a tiny Bluetooth adapter, the Myo Armband wirelessly transmits data to the computer, capable of acquiring sEMG signals at a sampling rate of 200 Hz.

JY901 module (WIT, China) integrates a high-precision gyroscope, accelerometer, and geomagnetic field sensor. It employs a high-performance microprocessor along with an advanced dynamic solution and a Kalman dynamic filtering algorithm to quickly solve the current real-time motion attitude of the module. It supports two types of digital interfaces: serial port and I²C. The output rate is adjustable from 0.2 to 200Hz.

The CYMH-1 (ChengYing, China) is a micro planar weighting sensor for applications requiring minimal space. Compared to thin-film resistor-based sensors, the CYMH-1 provides enhanced stability. It collects analog signals that can be sampled by the microcontroller.

C. Exoskeleton Design and Control

Fig. 2 shows the diagram of the GP-ULE device. The mechanical structure of the GP-ULE comprises four main components: shoulder, upper arm, forearm, and motor base. There is one active DoF at the elbow joint and two passive DoFs at the shoulder joint. The GP-ULE device is attached to the user's body using two adjustable fabric straps. The elbow joint rotation is realized through a brushless motor (Maxon EC 22), which is coupled with a planetary gearhead (Maxon GP 22 HP) and an incremental encoder (Maxon MR M-512). A specialized servo controller (ESCON 50/5, Maxon) is used to control the motor.

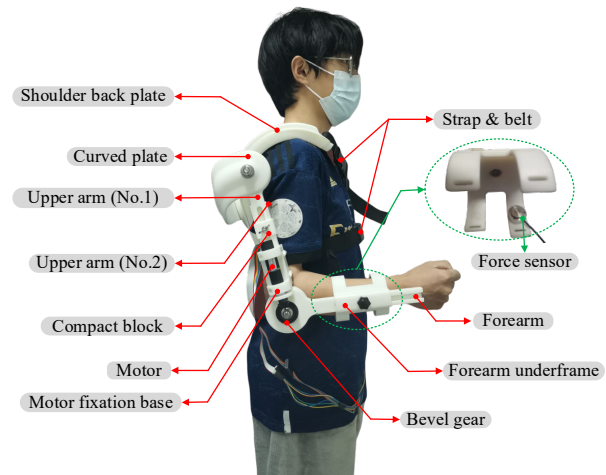


Fig. 2. The illustration of GP-ULE.

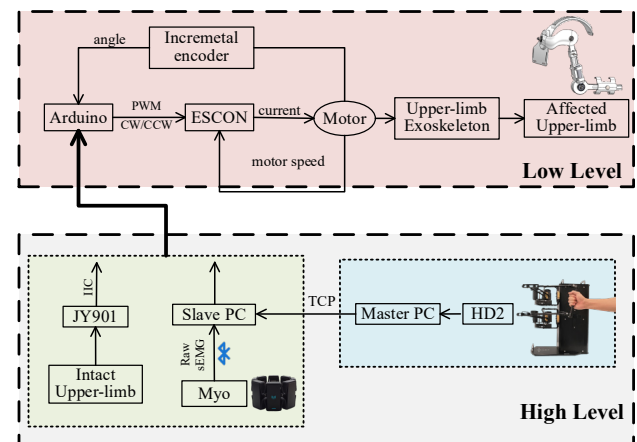


Fig. 3. The embedded system of the GP-ULE device.

The embedded system includes high-level and low-level control, as shown in Fig. 3. The high-level control is implemented in MATLAB/Simulink. It handles tasks such as HD² angle acquisition, transmission in telerehabilitation, and the sEMG-based prediction in bilateral rehabilitation. Data

> REPLACE THIS LINE WITH YOUR MANUSCRIPT ID NUMBER (DOUBLE-CLICK HERE TO EDIT) <

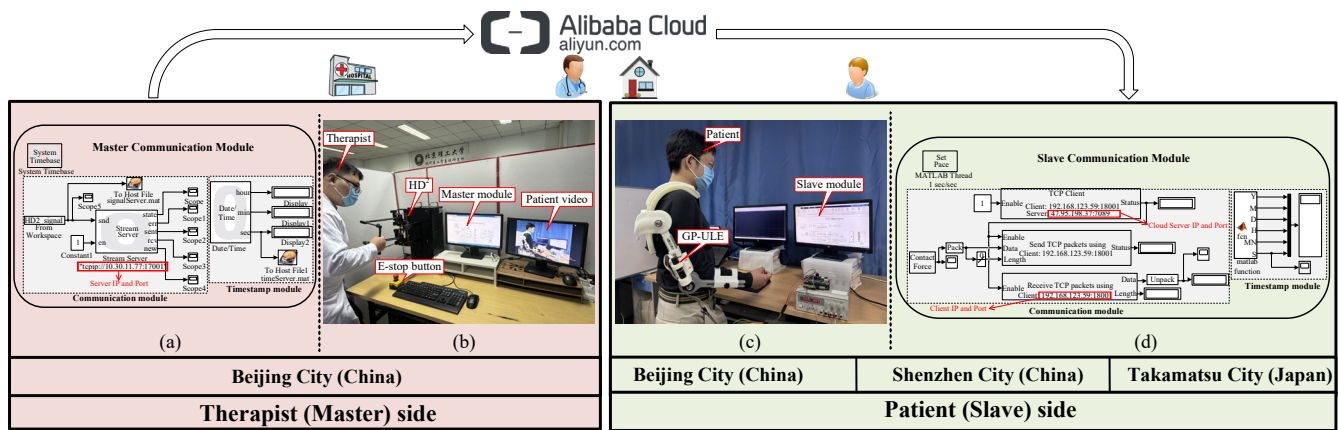


Fig. 4. The experimental setup and overall communication module. (a) master communication module in Simulink (b) master side's experimental setup (c) slave side's experimental setup (d) slave communication module in Simulink.

from MATLAB is transmitted to the microcontroller at 115200 bps via a serial port. The low-level controller includes an outer-loop controller (that is, the position controller) and an inner-loop controller (that is, the velocity controller), which is realized in Arduino Mega 2560. The outer controller is based on the tracking error between the angles of the healthy side and the motor. A reference velocity for the inner loop is created through the built-in Hall sensor of the servo motor.

D. Cloud Communication-based Telerehabilitation

This section introduces the CBTR subsystem of the HB-ULR system, as illustrated in Fig. 4. Fig. 4 (b) and Fig. 4 (c) depict the experimental setup. One subject (as a therapist) manipulates the HD² to remotely deliver rehabilitation treatment to another subject (as a patient) wearing the GP-ULE. The therapist can also perceive the interaction force between the affected limb and the robot in real time. Fig. 4 (a) and Fig. 4 (d) show the communication module of the master side and the slave side in Simulink. The feasibility of cloud-based teleoperation and cross-LAN communication is analyzed.

1) Feasibility of Cloud-based Teleoperation

In the CBTR subsystem, the data transmission method should be determined first, followed by an evaluation of time delay and transmission error. In the data transmission process, the master-side controller (HD²) captures the therapist's motion angles, which are then transmitted to the slave side via a cloud server. Once the slave side interprets the data, the GP-ULE executes corresponding movements. Simultaneously, the contact force between the GP-ULE and the affected limb is fed back from the master side to the slave side.

According to signal transmission mode, communication systems can be categorized into wired and wireless communication systems. Wired communication includes technologies such as Ethernet cables and fiber-optic connections, while wireless communication encompasses Wi-Fi, Bluetooth, mobile communication systems, etc. In our study, the long-distance telerehabilitation training requires stable and uninterrupted signals, making Ethernet the preferred choice for data communication.

Since the HD² operates within the MATLAB/Simulink

environment, the tele-rehabilitation system involved in this study is also implemented in the MATLAB/Simulink operating environment. Given the requirements for connection stability and implementation complexity, the signal transmission of the cloud-based teleoperation employs a socket communication mechanism using the TCP protocol. A socket is defined by an IP address and a port number, uniquely identifying each separate data stream. Ali Cloud is chosen as the cloud platform with a configuration of 2 cores and 2 GB memory, a bandwidth of 3 Mbps, and the Windows Server 2012 R2 operating system.

2) Cross-LAN Communication based on a Cloud Server

a) TCP Intranet Penetration

Both the master PC and slave PC typically use intranet IP addresses. Consequently, intranet penetration is necessary between the cloud server and the master PC. The core concept of intranet penetration involves “mapping” and “forwarding”. The port of an intranet device is mapped to the port of a public network device for traffic forwarding.

Fast Reverse Proxy (FRP) is adopted in this study to implement intranet penetration. FRP is a high-performance reverse proxy application that enables penetration of internal network easily, providing services to the external network and supporting protocols such as TCP, HTTP, and HTTPS. The principle behind this tool involves establishing a connection between a terminal on the external network and one requiring intranet penetration. It then forwards the services from the intranet terminal to the external network terminal.

b) GNSS Clock Synchronization

To accurately measure the communication delay between the master side and the slave side, precise clock synchronization is required. Commonly used methods for clock synchronization include Network Time Protocol (NTP) and Global Navigation Satellite System (GNSS). The NTP protocol can achieve an accuracy of approximately 1 ms within a local area network (LAN), but only around 50–500 ms over a wide area network (WAN). Therefore, NTP is insufficient for achieving millisecond-level synchronization in cloud-based teleoperation systems. Therefore, GNSS is used to synchronize the clock of the master PC and the slave PC.

The USB GPS Receiver UB-353 (Chipset: M8030-KT, U-

> REPLACE THIS LINE WITH YOUR MANUSCRIPT ID NUMBER (DOUBLE-CLICK HERE TO EDIT) <

blox, Switzerland) is adopted in this study. The GPS Receiver follows the NMEA-0183 standard protocol. It features a compact, self-contained, and waterproof design with a non-slip base for secure placement. The GPS Receiver generates a Pulse Per Second (PPS), where the rising edge precisely marks the beginning of each UTC second. This PPS signal offers an accuracy of tens of nanoseconds without any cumulative error.

Both the master and slave PC are connected to individual GPS receivers, allowing each system to obtain highly accurate time stamps and ensuring mutual synchronization. The u-center is a GNSS evaluation software designed for U-blox M8, M9, F9, and legacy GNSS products. It is used for the basic configuration of the GPS Receiver. NMEATime (VisualGPS, LLC, USA) automatically synchronizes the PC clock with the time provided by a GPS receiver connected via the serial port, enabling the PC to remain synchronized to an atomic time standard.

c) Establishment of Communication Channel

Based on the TCP-based intranet penetration and the GNSS clock synchronization, the communication model is built in Simulink, as shown in Fig. 4 (a) and Fig. 4 (d). This Simulink model includes the master and slave components. On the master side, the communication module employs the “Stream Server” module from QuaRC, while the slave side utilizes the “TCP Client” module. Timestamps are added on both sides to calculate the communication delay between the master PC and the slave PC. On the slave PC, the “MATLAB function” module is adopted to retrieve the system time, while the master PC employs the “Data/time” block from QuaRC for the same purpose.

E. sEMG-driven Subject-independent Bilateral Training using Transfer Learning

This section introduces the sEMG-SIBR subsystem of the HB-ULR system, as shown in Fig. 5. The intact limb drives the affected limb assisted by the GP-ULE to carry out symmetric bilateral movements. The following describes the specific processes, including the acquisition of sEMG signals, signal preprocessing, and the subject-independent prediction of continuous movements. The transferred model based on pretrained CNN-LSTM is used for subject-independent estimation of continuous motion.

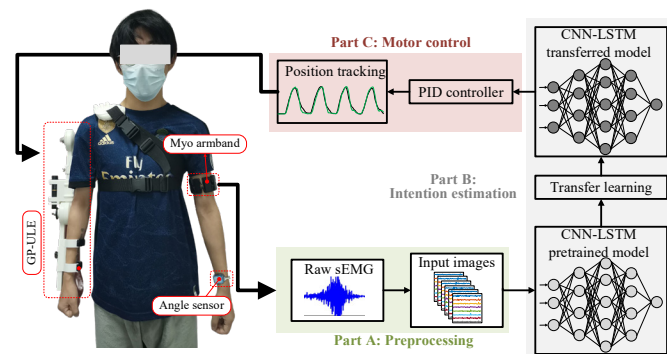


Fig. 5. The overall flow chart of the sEMG-SIBR system.

1) sEMG Acquisition

This study involved 10 subjects (marked as S1-S10),

including 5 males and 5 females, with an average age of 25.4 years. All participants are right-handed and free of skeletal and neurological diseases. All participants gave their permission to be part of this study. All experimental procedures follow the Declaration of Helsinki on Medical Research involving Human Subjects. The offline sEMG data were acquired through the Myo armband. The JY901 was attached to the forearm to record motion angles, which serve as the target values. The sampling frequency is set to 20 Hz.

Each volunteer wore the MYO armband and IMU on the left arm, ensuring that the 5th or 6th channels of the armband cover the corresponding area of the biceps, as shown in Fig. 5. Then, continuous elbow flexion-extension movements are performed. Each collection lasted 60 seconds, and a total of five trials were conducted per subject. After each collection, participants returned to a relaxed state. To avoid muscle fatigue affecting the signal quality, a 2-minute rest period was given between each collection.

2) Signal Preprocessing

Since raw sEMG signals are often interfered with noise, the preprocessing of the offline data is necessary. A 20 Hz high-pass filter is used to eliminate the low-frequency noise. Due to the non-stationary nature of sEMG signals, a sliding window approach is adopted to maintain signal stability. Fig. 6 illustrates the schematic diagram of the time window segmentation process. The sliding window is 250 ms with an overlap of 200 ms, satisfying the <300 ms latency requirement for real-time control [22]. To align the sampling points between the Myo armband and JY901 sensor, the angles obtained through the JY901 sensor are also segmented into 250-ms windows with an overlapping of 200 ms.

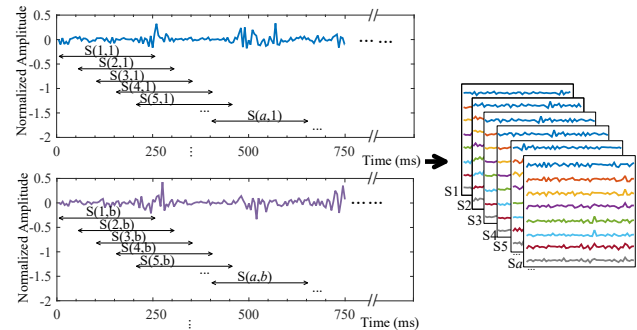


Fig. 6. The conversion of sEMG signals to sEMG images via an overlapping sliding window. $S(a,b)$ represents the a^{th} segment of the sEMG signal from the b^{th} channel. S_a represents the a^{th} segment of sEMG signals from all 8 channels.

3) Subject-independent Continuous Angle Prediction

Unlike traditional shallow neural networks, which rely on artificially extracted features, a deep neural network can transform the feature representation into a new feature space via layer-by-layer feature transformation. CNN can be adopted to realize the feature extraction and estimation of motion intention. Given that sEMG signals are time-related, LSTM combined with CNN to extract features is more effective, that is, CNN-LSTM. This model is used to estimate the continuous movements of the elbow joint. Based on the pre-trained CNN-

> REPLACE THIS LINE WITH YOUR MANUSCRIPT ID NUMBER (DOUBLE-CLICK HERE TO EDIT) <

LSTM model, transfer learning is further combined to realize the subject-independent estimation of continuous motion.

The sEMG-SIBR system includes three phases: offline training, transfer learning, and real-time intention estimation, as illustrated in Fig. 7. All three stages involve preprocessing, window segmentation, and sEMG image conversion. Transfer learning is conducted based on the pre-trained CNN-LSTM model from the offline training phase. Specifically, it utilizes 1-minute data from a new user to fine-tune the model, and finally, the real-time intention estimation is carried out based on the model after transfer learning.

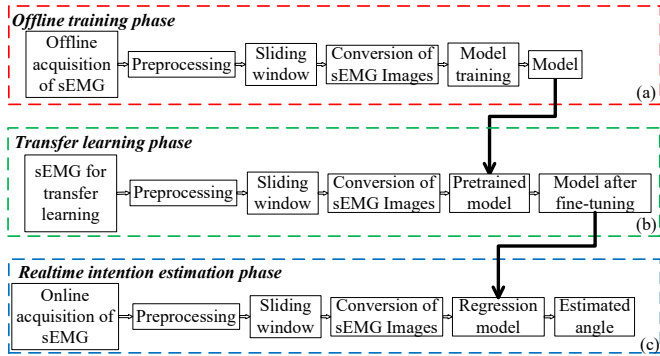


Fig. 7. The three phases in the sEMG-SIBR system. (a) offline training phase (b) transfer learning phase (c) real-time intention estimation phase.

a) Offline Training: The offline training (Fig. 7a) is based on previously collected sEMG data. Specifically, data from subjects S1–S7 are used for training, while data from subjects S8–S10 are reserved for testing. The structure of CNN-LSTM is shown in Fig. 8, with an input dimension of 50×8 (corresponding to sEMG images) and a single output neuron representing the predicted motion angles. The input to the CNN-LSTM model is the sEMG images converted from sEMG signals via an overlapping sliding window approach. This model has 15 layers in total, including one convolutional layer, two LSTM layers, two fully-connected layers, and one regression output layer.

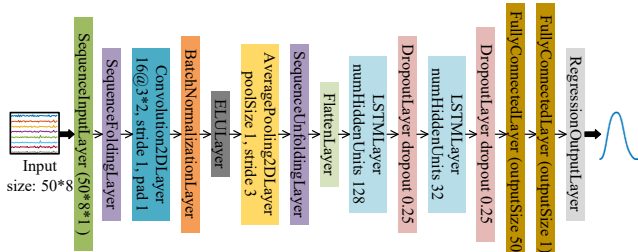


Fig. 8. The layer illustration of the CNN-LSTM model.

During training, the dataset is randomly divided into a training set (70%) and a validation set (30%). The Adam optimization algorithm is employed for network training, known for its adaptive learning rate adjustment, which accelerates convergence and performs well on high-dimensional data. Specific settings include a maximum of 20 epochs, with each batch containing 16 samples. The initial

learning rate is set to 0.001, and a piecewise learning rate schedule is adopted to reduce the learning rate by a factor of 0.8 every 20 epochs, enhancing training stability. To mitigate the risk of gradient explosion, a gradient clipping mechanism is applied with a threshold value of 1. Additionally, an L2 regularization term with a coefficient of 0.001 is incorporated to improve model generalization.

b) Transfer Learning: Transfer learning is a well-known topic in machine learning, commonly used to adapt models trained on one domain to new but related tasks or subjects. In this study, the widely adopted fine-tuning approach is employed to transfer knowledge from the pre-trained CNN-LSTM model to a new subject. Specifically, the network architecture of the CNN-LSTM model remains unchanged during the transfer learning phase, ensuring consistency with the original model structure. To calibrate the model for a new subject, the initial weights are transferred from the pre-trained model and then fine-tuned using one-minute offline data collected from the new user. This efficient adaptation strategy enables the model to quickly adjust to the characteristics of the new subject while leveraging the previously learned features. The steps of the transfer learning are shown in Fig. 7(b).

c) Real-time Intention Estimation: The real-time intention estimation is based on the fine-tuned CNN-LSTM model. In this stage, all procedures are performed in real-time, as shown in Fig. 7c. The predicted angles are obtained in real-time, and the whole estimation process corresponds to the high-level control realized in MATLAB. The estimation results are then transmitted to Arduino through serial communication, corresponding to the low-level control. Finally, the GP-ULE control can be realized in real time based on both the high-level and low-level control loops.

F. Evaluation Criteria

In the evaluation of the telerehabilitation system, time delay and angle error are analyzed. Mean Absolute Error (MAE), Root Mean Square Error (RMSE), and Correlation Coefficient (R) are adopted to evaluate the angular tracking error. MAE (defined in (1)) is the average of all absolute errors between the target and true angles. RMSE (defined in (2)) is the standard deviation of the target and true angles. R (defined in (3)) is a number between -1 and 1 that indicates the correlation between the target and true angles. For the sEMG-SIBR subsystem, the criteria of MAE, RMSE, and R are also adopted to evaluate the prediction effect of continuous motion.

$$MAE = \frac{1}{N} \sum_{i=1}^N |y_i - x_i| \quad (1)$$

$$RMSE = \sqrt{\frac{1}{N} \sum_{i=1}^N (y_i - x_i)^2} \quad (2)$$

$$R = \frac{\sum_{i=1}^N (x_i - \bar{x})(y_i - \bar{y})}{\sqrt{\sum_{i=1}^N (x_i - \bar{x})^2 \sum_{i=1}^N (y_i - \bar{y})^2}} \quad (3)$$

Where x_i represents the master side's motion angles at the i th data point, \bar{x} is the average value, y_i means the slave side's motion angles at the i th data point, \bar{y} is the average value, and N is the total number of data points.

> REPLACE THIS LINE WITH YOUR MANUSCRIPT ID NUMBER (DOUBLE-CLICK HERE TO EDIT) <

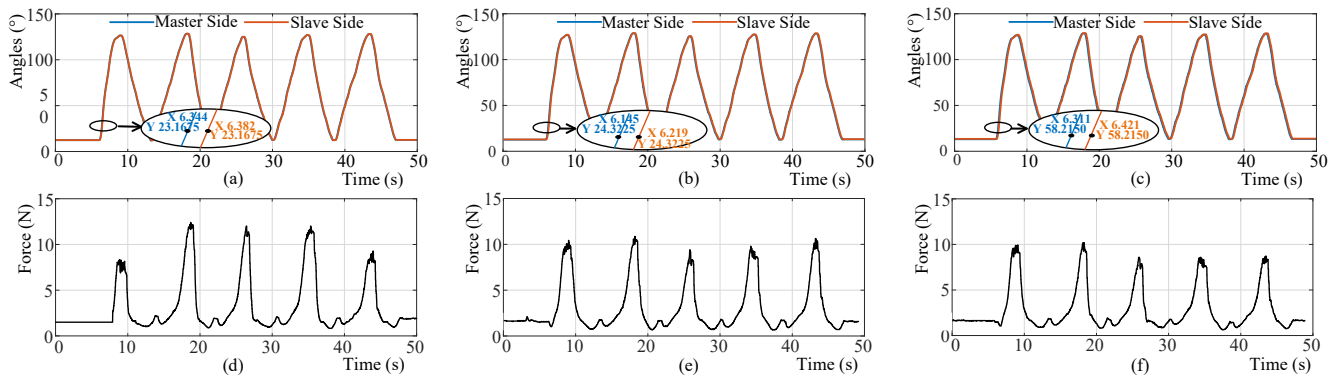


Fig. 9. Motion angles and contact force of master side (in Beijing City) and slave side in Beijing City (a)(d) slave side in Beijing City (b)(e) slave side in Shenzhen City (c)(f) slave side in Takamatsu City.

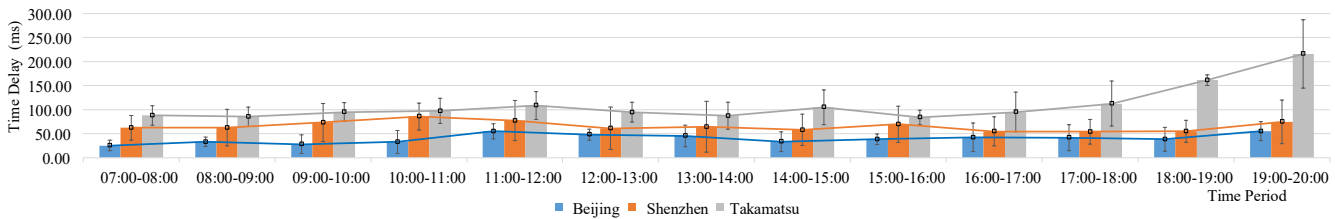


Fig. 10. Histogram of average delay of data transmission between master side and slave side.

III. SYSTEM EXPERIMENT DESCRIPTION

The proposed HB-ULR system includes the CBTR and the sEMG-SIBR subsystem. These two sub-systems operate independently and support distinct rehabilitation modes: remote training and bilateral training. The therapist-in-the-loop CBTR can provide professional training guidance that enhances the overall functionality of the HB-ULR framework. Therefore, both platforms are implemented and experimentally validated. The experiments are carried out for both platforms, respectively. The corresponding experimental setups are described below.

A. Telerehabilitation based on Cloud Communication

In the CBTR platform, the master side is located in Beijing City (China), while the slave side includes three regions: Beijing City (China), Shenzhen City (China), and Takamatsu City (Japan). A human operator (serves as a therapist) operates the handle of the HD² haptic device (the therapist-side robot in the implemented CBTR platform). The motion signals are transmitted to the slave side through a cloud server, which controls the exoskeleton to assist the patient's movement. Simultaneously, the contact force between the patient's affected limb and the rehabilitation exoskeleton is fed back from the slave side to the master side. For each of the three slave positions, five-times experiments are performed per hour (from 7:00 am Beijing time to 8:00 pm Beijing time). Each experiment is conducted for 50 seconds, during which all relevant data are recorded.

B. sEMG-based Subject-independent Bilateral Training

The sEMG-SIBR platform is distinct from the cloud-based telerehabilitation platform. In this platform, the unaffected limb drives the affected limb through decoding sEMG signals,

which is assisted by the GP-ULE to carry out symmetric movements. A regression model based on CNN-LSTM is trained using offline data. Subsequently, transfer learning adapts the model using a new user's one-minute data. Finally, the motion intention of the intact limb, predicted by the transferred model, drives the GP-ULE to assist the movements of the affected limb. During both the offline and real-time phases, each participant performs continuous elbow flexion-extension movements following the predefined sEMG acquisition protocol.

IV. EXPERIMENTAL RESULTS

This section presents the experimental results and performance analysis to evaluate the effectiveness of the proposed system. For the performance evaluation of the CBTR platform, the communication delay, the position tracking, and the contact force are analyzed in turn. For the prediction performance evaluation of the sEMG-SIBR platform, the results of the offline training and the real-time estimation are analyzed in turn.

A. Performance Evaluation of the CBTR Subsystem

As previously described, the CBTR platform enables therapists to provide direct kinesthetic guidance to patients with stroke. Additionally, the therapist can perceive the contact force generated during the interaction between the affected limb and the rehabilitation exoskeleton. Fig. 9(a)-(c) show the motion trajectories over time, with the slave side located in Beijing, Shenzhen, and Takamatsu, respectively. The blue line represents motion signals from the therapist side, while the orange line represents motion signals from the patient side. Fig. 9(d)-(f) shows the contact force. In this session, the performance of the CBTR platform is analyzed.

> REPLACE THIS LINE WITH YOUR MANUSCRIPT ID NUMBER (DOUBLE-CLICK HERE TO EDIT) <

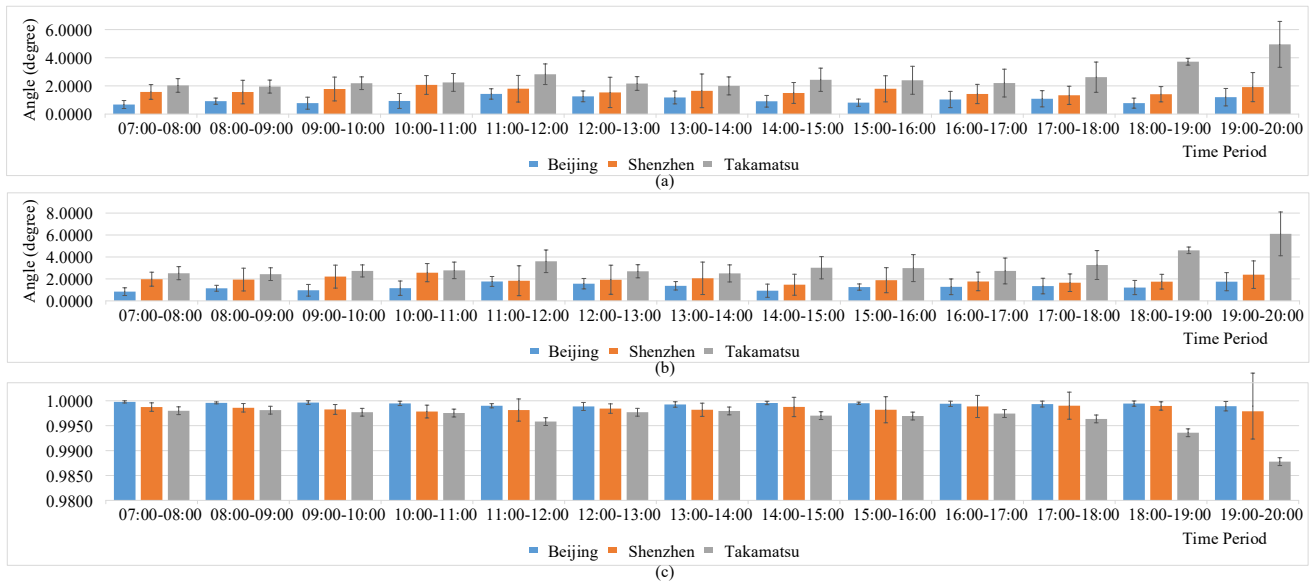


Fig. 11. Histogram of tracking effect between master side and slave side. (a)MAE (b)RMSE (c)R.

Latency is a critical factor in the tele-rehabilitation process. It affects both the smoothness of user–therapist interactions and the overall quality of rehabilitation outcomes. First, in rehabilitation activities requiring immediate feedback, any noticeable delay can undermine this immediacy. As a result, users may struggle to adjust their movements based on the received feedback. This is especially relevant in systems using haptic feedback, where latency reduces the realism of the interaction and the system’s responsiveness, ultimately affecting user engagement and satisfaction. Second, from a perspective of rehabilitation effectiveness, latency can significantly reduce the accuracy and overall efficacy of the training process. The real-time correction of erroneous movements is a critical component of rehabilitation training. Delays can lead to delayed corrections, which may degrade the quality of rehabilitation even causing secondary injuries. Therefore, the performance of the CBTR is evaluated in terms of communication delay, master/slave position tracking, control delay, and contact force, as follows.

1) Communication Delay

To quantitatively analyze the communication delay between master side and slave side, the time delay of each experiment is visualized in Fig. 10. The figure displays histograms showing average value (AVE) and standard deviation (STD) of time delay recorded per hour (from 7:00 am Beijing time to 8:00 pm Beijing time). As summarized in TABLE I, when the slave location is Beijing, the maximum time delay is 54.80 ms, the minimum time delay is 25.20 ms, and the average time delay is 38.43 ms. When the slave location is Shenzhen, the maximum time delay is 85.60 ms, the minimum time delay is 53.80 ms, and the average time delay is 66.45 ms. When the slave location is Takamatsu, the maximum time delay is 215.80 ms, the minimum time delay is 83.60 ms, the average time delay is 109.80 ms, and the time delay increases significantly after 6 pm (Beijing time). Whether the slave location is Beijing, Shenzhen, or Takamatsu, its

communication delay meets the requirements, less than 300 ms.

TABLE I
THE TIME DELAY OF DATA TRANSMISSION BETWEEN THE MASTER SIDE AND THE SLAVE SIDE

	Time Delay (ms)		
	Beijing	Shenzhen	Takamatsu
MIN	25.20	53.80	83.60
MAX	54.80	85.60	215.80
Ave	38.43	66.45	109.80

The timestamp resolution from the Windows operating system is limited to a maximum of 10 or 15 ms, depending on the underlying hardware configuration. The master PC adopts QUARC to stabilize the clock frequency and achieve a timestamp accuracy of 1 ms. However, the slave PC has a timestamp accuracy of 10 or 15 ms, leading to an approximate 10 ms clock synchronization error between the master PC and the slave PC.

2) Master-Slave Position Tracking

In addition to communication delay, the master-slave position tracking precision is discussed in this section. Quantitative evaluation of the tracking error is performed using MAE, RMSE, and R, as illustrated in Fig. 11(a)–(c), which present the histograms of tracking error. As summarized in TABLE II, the tracking performance between the master side and the slave side is recorded. Using MAE as an example, the tracking error for the three different slave locations is analyzed. For the slave in Beijing, the tracking error ranges from 0.6782° to 1.4294°, with an average of 0.9989°. For the slave in Shenzhen, the tracking error ranges from 1.3323° to 2.0685°, with an average of 1.6421°. For the slave in Takamatsu, the tracking error ranges from 1.9518° to 4.9508°, with an average of 2.5958°. Lower values of MAE and RMSE indicate better tracking performance, while higher values of R reflect stronger correlation between the master and slave movements.

> REPLACE THIS LINE WITH YOUR MANUSCRIPT ID NUMBER (DOUBLE-CLICK HERE TO EDIT) <

TABLE II
THE TRACKING EFFECT BETWEEN MASTER SIDE AND SLAVE SIDE

Index		Beijing	Shenzhen	Takamatsu
MAE	MIN	0.6782	1.3323	1.9518
	MAX	1.4294	2.0685	4.9508
	Ave	0.9989	1.6421	2.5958
RMSE	MIN	0.8404	1.4745	2.4317
	MAX	1.7702	2.5673	6.1050
	Ave	1.7702	1.9556	3.2277
R	MIN	0.9989	0.9978	0.9878
	MAX	0.9998	0.9990	0.9981
	Ave	0.9994	0.9985	0.9963

3) Control Delay

In the therapist-in-the-loop tele-rehabilitation system, the entire control process begins with the master PC transmitting commands to the slave PC. The slave PC then transmits these commands to the lower-level controller via a serial port. The lower-level controller executes the commands by driving the motors, which activate the exoskeleton to assist the patient's limb movement and provide force feedback. The force feedback is collected by the lower-level controller and sent back to the slave PC via the serial port, and subsequently transmitted to the master PC, enabling therapists to perceive the interaction force in real time. The communication delay between the master PC and the slave PC is analyzed in the "Communication Delay" subsection. Accordingly, this subsection focuses on the serial port communication delay and the control delay associated with executing commands and providing haptic feedback.

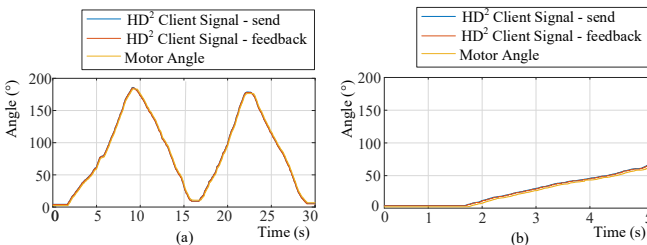


Fig. 12. Motion angles between Client PC and lower-level controller (a) motion angles (b) partial zoom

TABLE III

THE TIME DELAY BETWEEN THE CLIENT PC AND MICROCONTROLLER

	Delay of motor control and serial transmission (ms)	Delay of serial transmission (ms)	Delay of motor control (ms)
1 st	226	17	209
2 nd	205	16	189
3 rd	213	18	195
4 th	223	19	204
5 th	198	18	180
Ave	213.0	17.6	195.4

Fig. 12 shows the motion angles between the slave PC and the microcontroller. The blue line represents the command signal received from the master PC, the red line represents the client signal received from the microcontroller, and the orange line represents the motor angle recorded by the slave PC. Both the total delay (including motor control and serial transmission) and the serial transmission delay are recorded. Thus, the delay of motion control can be calculated, as

summarized in Table III. The average delay of serial transmission is 17.6 ms, while the average delay of motor control is 198.6 ms. Given that the communication delays across the three locations range from 30 to 100 ms, the total system delay remains below 300 ms [22].

4) Contact Force

Fig. 9(d)-(f) show the contact force between the patient's affected limb and the rehabilitation exoskeleton. This force is transmitted to the master side through a cloud server, allowing therapists to intuitively perceive it through the handle of HD². The magnitude of the interaction force reflects the severity of hemiplegia and typically decreases as rehabilitation progresses.

Here, a comparative experiment is performed to assess differences in interaction forces. Experiment one was conducted on patients with complete hemiplegia (normal people simulate this condition without voluntary movements at all). Experiment two was conducted on normal people. The results, shown in Fig. 13, clearly demonstrate the difference in the magnitude of the interaction force in the two situations. Therefore, through the feedback of this force, therapists can assess the severity of hemiplegia during the telerehabilitation process. Furthermore, therapists can provide guidance for patients to perform sEMG-SIBR independently at home.

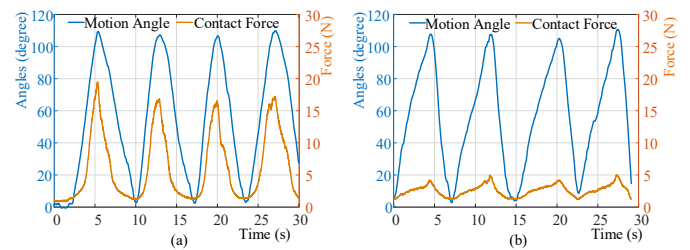


Fig. 13 Comparison of the contract force. (a) Without voluntary motion (b) With voluntary motion

B. Prediction Performance of the sEMG-SIBR

Based on the proposed sEMG-SIBR platform, the affected side of the patient is driven by the GP-ULE, which is controlled using sEMG signals from the patient's intact limb. The accuracy of sEMG decoding directly affects the outcome of bilateral rehabilitation. This section presents the analysis of the CNN-LSTM regression model with and without transfer learning under both offline and real-time situations. The estimation results obtained with and without transfer learning in offline situations are compared. Quantitative assessments are performed using the metrics MAE, RMSE, and R.

1) Offline Training and Estimation

For all 10 subjects (S1-S10), data from the first seven (S1-SS7) are used for model training, while data from the remaining three (S8-S10) serve as the additional test set. The quantitative evaluation results obtained with and without transfer learning are recorded in Table IV. Fig. 14 shows the offline angle estimation results with and without transfer learning. Fig. 14(a)-(c) present the offline angle prediction results for subjects S8-S10, respectively. These figures highlight the differences in prediction performance across subjects S8-S10. Fig. 14(a)-(c) demonstrate the inter-subject variability. For subject S8, the estimation performance without

> REPLACE THIS LINE WITH YOUR MANUSCRIPT ID NUMBER (DOUBLE-CLICK HERE TO EDIT) <

TABLE IV
THE QUANTITATIVE EVALUATION WITH AND WITHOUT TRANSFER LEARNING

Subject	Index	1 st time		2 nd time		3 rd time	
		Without TL	With TL	Without TL	TL	Without TL	TL
S8	MAE	12.8540	6.7763	10.3138	6.8981	13.1963	9.3246
	RMSE	15.1952	9.1089	13.5687	9.0546	15.1348	12.0140
	R	0.9250	0.9754	0.9128	0.9612	0.9299	0.9558
S9	MAE	13.0131	7.0417	8.2149	7.3154	9.8323	5.7868
	RMSE	15.3746	9.4837	10.8444	9.0253	11.9224	7.7910
	R	0.9274	0.9724	0.9545	0.9685	0.9513	0.9792
S10	MAE	11.3080	8.1728	7.5937	5.6038	12.2877	9.6573
	RMSE	15.2089	11.2321	10.3448	7.0407	16.4640	12.1203
	R	0.9347	0.9644	0.9559	0.9796	0.8811	0.9355

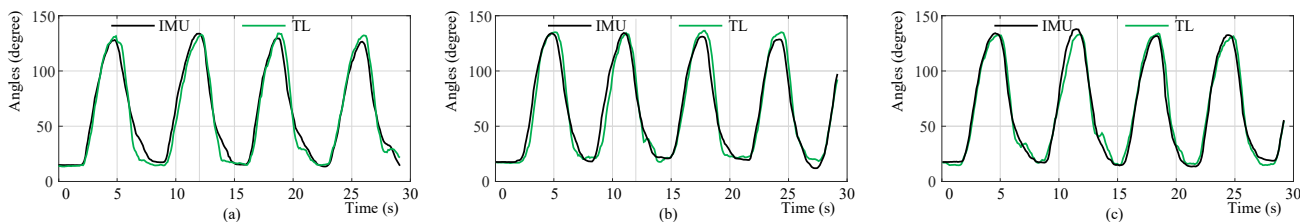


Fig. 15. The results of the real-time estimation of motion angles. (a) the results of the 1st time experiment (b) the results of the 2nd time experiment (c) the results of the 3rd time experiment.

transfer learning is the lowest. For subject S9, the prediction performance without transfer learning is moderate. For subject S10, the prediction performance without transfer learning is the highest. Regardless of subjects (S8–S10), the prediction performance is improved through the CNN-LSTM model with transfer learning. The transferred model consistently improves prediction accuracy, demonstrating its effectiveness in addressing inter-subject variability.

line represents the IMU-measured motion angles, while the green line represents the model-predicted angles using the transfer-learned CNN-LSTM model. In contrast to the offline phase, real-time prediction requires additional evaluation of time delay, along with MAE, RMSE, and R, as summarized in Table V. The time delays between the angles from the attitude sensor and the estimated angles are 50 ms, 0 ms, and 0 ms across the three trials, indicating minimal overall latency. This low latency can be attributed to the fact that sEMG signals typically occur 30–150 ms prior to actual movement onset. Additionally, the utilization of sliding windowing and filtering techniques introduces a predictive bias in the signal processing, effectively giving the model a forward-looking tendency. The MAE remains below 8°, and the RMSE stays within 10°, demonstrating the effectiveness of the model in suppressing the inter-subject variability.

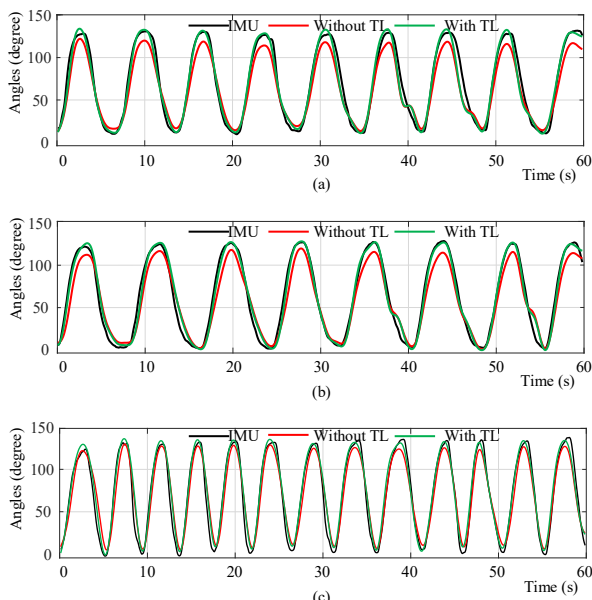


Fig. 14. The offline angle estimation with and without transfer learning. (a) subject S8 (b) subject S9 (c) subject S10.

2) Real-time Estimation of Motion Angle

Based on the offline training and prediction, the CNN-LSTM model after transfer learning is applied to real-time estimation. Fig. 15(a)–(c) presents the real-time motion angle estimation results from three separate experiments. The black

TABLE V
THE QUANTITATIVE EVALUATION OF THE REAL-TIME ANGLE ESTIMATION

Times	Index	Value
1 st	Time Delay	50 (ms)
	RMSE	9.6512 (°)
	MAE	7.2879 (°)
	R	0.9659
2 nd	Time Delay	0 (ms)
	RMSE	10.3943 (°)
	MAE	7.3983 (°)
	R	0.9608
3 rd	Time Delay	0 (ms)
	RMSE	7.9008 (°)
	MAE	6.1086 (°)
	R	0.9767

V. DISCUSSION

As shown in Table VI, the proposed rehabilitation system offers several advantages over existing systems: Firstly, the use of WAN enables broader coverage and higher data

> REPLACE THIS LINE WITH YOUR MANUSCRIPT ID NUMBER (DOUBLE-CLICK HERE TO EDIT) <

TABLE VI
THE COMPARISON WITH OTHER REHABILITATION SYSTEMS

	Communication mode	Home-based/Portability	Haptic feedback	sEMG-driven subject-independent
Yang et al. [20]	LAN	Yes	Yes	No
Liu et al. [4]	LAN	Yes	Yes	No
Patel et al. [11]	LAN	No	Yes	No
Chen et al. [21]	Bluetooth.	Yes	No	No
This study	WAN	Yes	Yes	Yes

transmission capacity compared to LANs or Bluetooth-based solutions. Secondly, the home-based nature of the system makes it suitable for deployment in home-based environments, significantly improving user convenience and accessibility. Additionally, the integration of haptic feedback plays a crucial role in enhancing user engagement and providing a more immersive rehabilitation experience. Finally, as an sEMG-driven system, it operates based on sEMG signals without requiring individualized calibration, thereby enhancing its generalizability and ease of use.

The above offline and online experiments verify the effectiveness of the subject-independent prediction using transfer learning. The performance of the proposed method with existing approaches is further presented. Compared to previous studies focused on estimating continuous elbow joint movements, this study addresses both the requirements of HB-ULR and subject-independent prediction. The comparison results of different methods are presented in Table VI. Compared to other methods, the proposed approach achieves the lowest RMSE (9.2666) and the highest R (0.9679), suggesting that transfer learning is effective in solving the inter-subject variability of sEMG signals.

TABLE VI
THE PREDICTION COMPARISON WITH OTHER STUDIES

	RMSE	R
Yang et al. [17]	20.4400	0.8940
Zhao et al. [22]	17.5900	0.9100
Ding et al. [23]	13.2209	0.8400
Li et al. [5]	15.2596	0.9290
This Study	9.2666	0.9679

In summary, this study demonstrates that the tele-rehabilitation system can provide low-latency and stable communication services across various regions, while the transferred CNN-LSTM prediction model can effectively deal with inter-subject variability. By integrating tele-training and bilateral training, a home-based rehabilitation system is constructed. Looking ahead, future research could focus on further optimizing the communication network to enhance the system's adaptability in diverse environments. This includes exploring edge computing solutions to reduce latency, implementing more robust data transmission protocols to ensure reliability in areas with unstable connectivity, and leveraging 5G or next-generation wireless technologies for improved bandwidth and coverage.

VI. CONCLUSION

In this paper, a HB-ULR system based on cloud-based teleoperation and sEMG-driven subject-independent bilateral

training is built. The CBTR subsystem implements master-slave control through cloud-based communication. The HD² device, operated by the therapist, serves as the master side, while the GP-ULE worn on the hemiplegic patient acts as the slave side. The sEMG-SIBR subsystem enables subject-independent motion estimation of the elbow joint using the transferred CNN-LSTM model. The effectiveness of the overall rehabilitation system is verified through experiments involving both subsystems, highlighting its potential for home-based rehabilitation applications.

REFERENCE

- [1] C. Tsao *et al.*, "Heart Disease and Stroke Statistics-2023 Update: A Report From the American Heart Association," *Circulation*, vol. 147, no. 8, pp. e93-e621, Feb. 2023, doi: 10.1161/cir.0000000000001123.
- [2] F. Xiong *et al.*, "Emerging Limb Rehabilitation Therapy After Post-stroke Motor Recovery," *Front. Aging Neurosci.*, vol. 23, no. 14, Mar. 2022, Art no. 863379, doi: 10.3389/fnagi.2022.863379.
- [3] C. Stinear, C. Lang, S. Zeiler and W. Byblow, "Advances and challenges in stroke rehabilitation," *Lancet Neurol.*, vol. 19, no. 4, pp. 348-360, Apr. 2022, doi: 10.1016/s1474-4422(19)30415-6.
- [4] Y. Liu, S. Guo, Z. Yang, H. Hirata and T. Tamiya, "A Home-based Tele-rehabilitation System With Enhanced Therapist-patient Remote Interaction: A Feasibility Study," *IEEE J. Biomed. Health. Inform.*, vol. 26, no. 8, pp. 4176-4186, Aug. 2022, doi: 10.1109/JBHI.2022.3176276.
- [5] H. Li, S. Guo, D. Bu, H. Wang and M. Kawanishi, "Subject-Independent Estimation of Continuous Movements Using CNN-LSTM for a Home-Based Upper Limb Rehabilitation System," *IEEE Robot. Autom. Lett.*, vol. 8, no. 10, pp. 6403-6410, Oct. 2023, doi: 10.1109/LRA.2023.3303701.
- [6] Y. Liu, S. Guo, Z. Yang, H. Hirata and T. Tamiya, "A Home-Based Bilateral Rehabilitation System With sEMG-based Real-Time Variable Stiffness," *IEEE J. Biomed. Health. Inform.*, vol. 25, no. 5, pp. 1529-1541, May 2021, doi: 10.1109/JBHI.2020.3027303.
- [7] E. Zasadzka *et al.*, "Application of an EMG-Rehabilitation Robot in Patients with Post-Coronavirus Fatigue Syndrome (COVID-19)-A Feasibility Study," *Int. J. Environ. Res. Public Health.*, vol. 19, no. 16, Jun. 2022, Art. no. 10398, doi: 10.3390/ijerph191610398.
- [8] C. Lambelet, M. Lyu, D. Woolley, R. Gassert and N. Wenderoth, "The eWrist — A wearable wrist exoskeleton with sEMG-based force control for stroke rehabilitation," 2017 International Conference on Rehabilitation Robotics (ICORR), London, UK, Jul. 2017, pp. 726-733, doi: 10.1109/ICORR.2017.8009334.
- [9] C. Lambelet, *et al.*, "Characterization and wearability evaluation of a fully portable wrist exoskeleton for unsupervised training after stroke", *J. Neuroeng. Rehabilitation*, vol. 17, no. 1, Oct. 2020, Art. no. 132, doi: 10.1186/s12984-020-00749-4.D.
- [10] Shi, W. Zhang and X. Ding, "A Review on Lower Limb Rehabilitation Exoskeleton Robots," *Chin. J. Mech. Eng.*, vol. 32, no. 74, Aug. 2019, Art. no. 2019, doi: 10.1186/s10033-019-0389-8.
- [11] S. Atashzar, M. Shahbazi, M. Tavakoli and R. Patel, "A Computational-Model-Based Study of Supervised Haptics-Enabled Therapist-in-the-Loop Training for Upper-Limb Poststroke Robotic Rehabilitation," *IEEE ASME Trans. Mechatron.*, vol. 23, no. 2, pp. 563-574, Apr. 2018, doi: 10.1109/TMECH.2018.2806918.
- [12] J. Bai, A. Song, and H. Li, "Design and Analysis of Cloud Upper Limb Rehabilitation System Based on Motion Tracking for Post-Stroke Patients," *Appl. Sci.* vol. 9, no. 8, Apr. 2019, Art. no. 1620, doi:10.3390/app9081620
- [13] C. Yang, S. Guo, Y. Guo and X. Bao, "Cloud Communication-Based Sensing Performance Evaluation of a Vascular Interventional Robot

> REPLACE THIS LINE WITH YOUR MANUSCRIPT ID NUMBER (DOUBLE-CLICK HERE TO EDIT) <

- System,” *IEEE Sens. J.*, vol. 22, no. 9, pp. 9005-9017, May 2022, doi: 10.1109/JSEN.2022.3160760.
- [14] B. Sheng, Y. Zhang, W. Meng, C. Deng, and S. Xie, “Bilateral robots for upper-limb stroke rehabilitation: State of the art and future prospects,” *Med. Eng. Phys.*, vol. 38, no. 7, pp. 587-606, Jul. 2016, doi: 10.1016/j.medengphy.2016.04.004.
- [15] Y. Chen, Z. Yang, and Y. Wen, “A Soft Exoskeleton Glove for Hand Bilateral Training via Surface EMG,” *Sensors*, vol. 21, no. 2, Jan. 2021, Art. no. 578, doi: 10.3390/s21020578.
- [16] J. Li *et al.*, “Motion intention prediction of upper limb in stroke survivors using sEMG signal and attention mechanism,” *Biomed. Signal Process Control*, vol. 78, Sep. 2022, Art no. 103981, doi: 10.1016/j.bspc.2022.103981.
- [17] Z. Yang, S. Guo, Y. Liu, H. Hirata, T. Tamiya, “An intention-based online bilateral training system for upper limb motor rehabilitation,” *Microsyst. Technol.*, vol. 27, pp. 211–222, Jun, 2021, doi: 10.1007/s00542-020-04939-x.
- [18] Y. Bouteraa, I. B. Abdallah and A. Elmogy, “Design and control of an exoskeleton robot with EMG-driven electrical stimulation for upper limb rehabilitation”, *Ind. Robot*, vol. 47, no. 4, pp. 489-501, May 2020, doi: 10.1108/IR-02-2020-0041.
- [19] HD² High-Definition Haptic Device, QUANSER. Canada, <https://www.quanser.com/products/hd2-high-definition-haptic-device/>.
- [20] Z. Yang, S. Guo, L. Ren, R. An, Y. Liu and M. Kawanishi, “S2-RTPIC: A State-Switching Remote Therapist Patient Interaction Control for Telerehabilitation,” *IEEE Trans. Industr. Inform.*, vol. 21, no. 1, pp. 366-375, Jan. 2025, doi: 10.1109/TII.2024.3452244.
- [21] J. Chen, D. Hu, W. Sun, X. Tu, and J. He, “A Novel Telerehabilitation System Based on Bilateral Upper Limb Exoskeleton Robot,” 2019 IEEE International Conference on Real-time Computing and Robotics (RCAR), Irkutsk, Russia, 2019, pp. 391-396, doi: 10.1109/RCAR47638.2019.9044072.
- [22] Y. Zhao, Z. Zhang, Z. Li, Z. Yang, A. A. Dehghani-Sanij and S. Xie, “An EMG-Driven Musculoskeletal Model for Estimating Continuous Wrist Motion,” *IEEE Trans. Neural Syst. Rehabilitation Eng.*, vol. 28, no. 12, pp. 3113-3120, Dec. 2020, doi: 10.1109/TNSRE.2020.3038051.
- [23] Q. Ding, G. Zhao and J. Han, “EMG-based Estimation for Multi-joint Continuous Movement of Human Upper Limb,” *Robot*, vol. 36, no. 4, pp.469-476, Jul. 2014, doi: 10.13973/j.cnki.robot.2014.0469.



Ruijie He (Student Member, IEEE) received the B.S. degree in Northeastern University, Liaoning, China, in 2021. And he is currently studying for his M.S. degree in Beijing Institute of Technology, Beijing, China.

He researches on exoskeleton rehabilitation robotic systems and sEMG signal processing for biomedical applications



Hanze Wang (Student Member, IEEE) received the B.S. degree in School Biomedical Engineering from Beijing Institute of Technology, Beijing, China, in 2021. And he is currently studying for his M.S. degree in Beijing Institute of Technology, Beijing, China.

He researches on exoskeleton rehabilitation robotic systems for biomedical applications.



Masahiko Kawanishi received the B.S. degree from the Faculty of Medicine, Kagawa Medical University, Takamatsu, Japan, in 1993.

He is currently a Lecturer with the Faculty of Medicine, Kagawa University. He has authored or coauthored more than 80 refereed journal articles and conference papers. His current research interests include the surgical techniques of neurosurgical operations and intravascular surgery system.



He Li (Student Member, IEEE) received the M.S. degree in School of Precision Instrument and Opto-Electronics Engineering from Tianjin University, Tianjin, China, in 2021. She is currently pursuing the Ph.D. degree in Beijing Institute of Technology, Beijing, China.

She has published 9 journal and conference papers. She researches on exoskeleton rehabilitation robots, sEMG signal processing, and tele-rehabilitation system.



Shuxiang Guo (Fellow, IEEE) received the Ph.D. degree in mechatronics and systems from Nagoya University, Nagoya, Japan, in 1995.

He is currently with both Kagawa University, Japan, and Beijing Institute of Technology, China. His current research includes biomimetic underwater robots, minimal invasive surgery robot systems, and rehabilitation robotics.

Dr. Guo is an Editor-in-Chief for the International Journal of Mechatronics and Automation.